Identification of novel Ras pathway genes using an inducible *Drosophila* tumor cell line

Research Thesis

Presented in partial fulfillment of the requirements for graduation *with research distinction* in Molecular Genetics in the undergraduate colleges of The Ohio State University

By

Peter Lyon

The Ohio State University

April 2016

Project Advisor: Professor Amanda Simcox, Department of Molecular Genetics

Table of Contents

Abstract

The oncogenic form of Ras signaling is associated with 30% of human cancers, including 90% of pancreatic tumors, was first genetically characterized in *Drosophila*. Subsequent genetic screens have identified many additional genes in the pathway. To identify novel candidates, we have conducted an *in vitro* screen using an inducible Ras oncogene in *Drosophila* tissue culture cells developed in our lab. This conditional cell line requires the control of oncogenic Ras^{V12} expression induced by GeneSwitch-Gal4 (GSR) for proliferation. Using RNAseq analysis, 363 gene transcripts were identified that were upregulated two-fold or greater by oncogenic Ras^{V12} expression. Of these, 91 candidate genes were tested further for functional analysis using RNAi in flies. Ubiquitous knock-down of 38 target genes caused death or decreased viability of the organism, suggesting their essential role, and depletion of another gene caused a wing phenotype. As the Ras pathway is known to play an important role in wing-vein patterning, I carried out tissue-specific knock-downs in the wing. I am characterizing further three genes whose depletion results in the most robust wing venation defects. Knock-down of *G protein gamma 30A* (*Gγ30A*), a G-protein subunit, in the wing causes extra vein phenotypes, consistent with a negative Ras pathway regulator. Knock-down of *CG12009*, a chitin-binding protein, and *CG31689*, an ABC transporter, in the wing causes loss of vein phenotypes, consistent with positive Ras pathway regulators.

Acknowledgements

I would like to thank the members of the Simcox Lab for mentoring and assisting me in my research over the last three years and for advice in the editing of this thesis (Dr. Sathiya Manivannan, Dr. Delphine Fagegaltier, Dr. Uyen Tram, Ashley Heinaman, and Geeta Palsule). Special thanks to Dr. Amanda Simcox for allowing me to be part of her lab for the past three years and for taking time to mentor me into a research scientist. I would like to thank Pelotonia for sponsoring my Pelotonia International Internship and for L. S. Shashidhara for allowing me to conduct research in his lab at IISER-Pune, and I am grateful for Sanket Nagakar (LSS Lab), who mentored me during my summer at IISER. I would like to thank Dr. Mark Seeger for serving on my committee. Finally, thank you to the College of Arts and Sciences for the Undergraduate Research Scholarship and to Pelotonia for the Undergraduate Research Fellowship to support my work.

Introduction

The conserved Ras protein, present in all animals, responds to growth factor signaling between cells. Ras is a membrane-bound G protein that functions as a molecular switch that converts signals from the cell membrane to the nucleus to control cell growth, differentiation and survival. Its mutated form is permanently active and behaves as an oncogene; cells will continuously grow and divide, giving rise to tumors. Oncogenic Ras is associated with 30% of human cancers, including 90% of pancreatic tumors. For this reason, it is imperative to identify all of the components of the Ras pathway, as these components could be used as therapeutic targets. The Ras pathway was first characterized in *Drosophila* (Simon *et al.* 1991) and *C. elegans* (Han and Stenberg 1990). Subsequent genetic screens have identified many additional components of the pathway validated in mammals. Given the high degree of conservation of core signaling pathways, and that genetic analysis can be carried out rapidly in *Drosophila*, this makes *Drosophila* a good model system to gain knowledge of the Ras pathway and apply it in mammals. My goal is to identify novel Ras pathway components that will not only better our knowledge of the pathway but also identify potential candidates for targeted therapy.

The Ras protein itself is a poor target for therapy (Downward, J. 2003 and Gysin, S. *et al.* 2011), so finding downstream Ras effectors and other targets involved in Ras protein synthesis will be of great importance. To this aim, our lab has developed a conditional *Drosophila* cell line in which cell growth and proliferation are under the control of an inducible form of oncogenic Ras^{V12}. The cell line takes advantage of the GeneSwitch-Gal4 system developed by the Keshishian group (Osterwalder *et al*. 2001 and Nicholson *et al*. 2008), in which Ras^{V12} expression can be induced by the RU486 drug in *Drosophila* tissue culture cells. In the presence of the RU486 drug, Gal4 activation induces Ras^{V12} and *GFP* expression. Without the drug, Gal4 is not activated and

cells lack *Ras*^{V12} and *GFP* expression. The system successfully lead to the establishment of primary cell cultures with *Act5C-GeneSwitch-Gal4* driving expression of *UAS-Ras*^{V12} and *UAS-GFP* in the presence of RU486 (Figure 1). Work in the lab has shown that cell proliferation is tightly controlled by this system, and only primary cultures treated with RU486 reached confluence and gave rise to continuous cell lines. Two independent cell lines (GSR2 and GSR6) were established that show drug-dependent proliferation (Figure 1A). Cells were incubated without RU486 for 8 days and then the drug was reintroduced, causing cell proliferation (Figure 1A). This shows that the GSR cells are still alive, yet in a dormant state in the absence of the drug, and depend on Ras^{V12} expression for proliferation. FACS analysis of the cell cycle profile of the GSR cells in the absence and presence of RU486 found that GSR cells without RU486 accumulate in G_0/G_1 phase, but remain viable and quickly reenter the cell cycle upon RU486 reintroduction (Figure 1B).

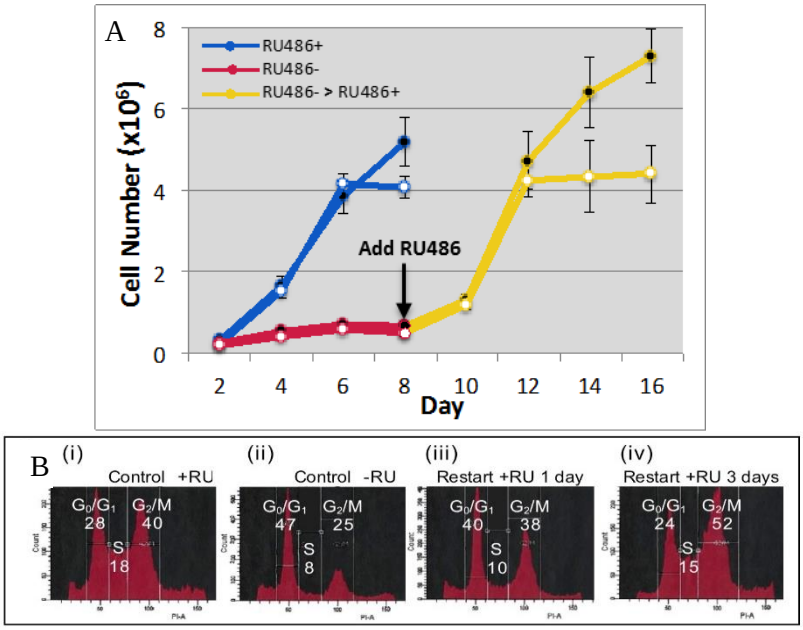

Figure 1: (A) GSR cells (GSR2 – black circles, GSR6 – white circles) cultured in the presence of RU486 proliferate (blue curve). GSR cells cultured without RU486 do not proliferate (red curve), but these same cells start to proliferate again after RU486 is reintroduced (yellow curve). (A. Heinaman, unpublished) (B) Control cells with (i) or without RU486 (ii) displayed different cell cycle profiles (both cultures had similar numbers of cells). When RU486 was added back to the cultures the cells entered the cell cycle and more cells in G_2/M were observed (iii and iv). # = % each stage. (Simcox Lab, unpublished)

A comparative analysis of gene expression in induced and non-induced cells was performed in the lab using RNAseq. 363 genes were found to upregulated upon Ras^{V12} induction in both the GSR2 and GSR6 cells. I conducted a selective genetic screen to validate these Ras-responsive gene candidates using reverse genetics. RNAi screens in *Drosophila* have proven valuable to identify novel components of signaling pathways (Jia *et al*. 2015 and Luo *et al*. 2015). Often, the *Drosophila* wing is used as a model for studying signaling, as the Egfr/Ras, Hh, Dpp, Wingless, and Notch signaling pathways all are required for proper vein patterning (reviewed in Blair 2007). For the Ras pathway, vein loss phenotypes are indicative of reduced Ras signaling and extra vein phenotypes are indicative of increased Ras signaling (Roch *et al*. 2002). The wing is also dispensable for viability and has a strict vein pattern that can easily be scored for alterations. Previous studies in our lab have successfully used the fly wing to characterize new regulators of the Egfr signaling (Butchar *et al.* 2012 and Jacobsen *et al.*, 2006). In fact, I have identified three genes that caused robust venation defects: *Gγ30A*, a potential negative Ras pathway regulator and *CG12009* and *CG31689*, potential positive Ras pathway regulators.

Materials and Methods

Fly stocks:

The following gene alleles and transgenes were used: *Dp(1;3)DC141*, *Dp(1;3)DC142*, *Dp(1;3)DC143*, *Dp(1;3)DC144*, *ap-Gal4*, *UAS-Egfr*, *UAS-yki*, *UAS-GFP*, $CG4096^{EPgy2}$, $Egfr^{Elp}$, $Ras85D^{e1B}$, *UAS-Dcr-2*, *Act5C-Gal4*, *en-Gal4*, *69B-Gal4*, *71B-Gal4*, and *vn-Gal4* (Austin *et al*. 2015).

For the screen in adult wings, a complete list of transgenic RNAi stocks obtained from the Harvard TRiP (Transgenic RNAi Project) and VDRC (Vienna *Drosophila* Research Center) collections is available in Appendix 2.

RNAseq of GSR cells:

Two runs of RNAseq were performed in the lab in both the presence and absence of RU486 for two independent inducible Ras^{V12} cell lines (GSR2 and GSR6) as well in a constitutive control line (Ras7). The RNAseq was performed on cells after 5 days in presence or absence of RU486. Expression data from the Ras7 line was used to eliminate transcripts upregulated due to the presence of RU486 alone.

Analysis of *CG4096* muatation generated by CRISPR/Cas9 targeting:

Cells expressing Cas9 via integration by RMCE (Recombinase-Mediated Cassette Exchange) were transfected with plasmid pU6-GuideRNA.CG4096 which contains the RNA targeting sequence against *CG4096* or with plasmid pU6-GuideRNA.SC which contains a control scrambled sequence. Genomic DNA from the cells was isolated 36h post-transfection. The region flanking the presumed CRISPR/Cas9 target site was amplified using Phusion (NEB)-mediated PCR and primers FP.CG4096.PCR and RP.CG4096.PCR. Mutations were detected using the PCR product

and a Surveyor Mutation Detection Kit (Transgenomic) by following the protocol that cuts at mismatched sequences resulting from CRISPR/Cas9-induced deletions or insertions. (Manivannan, S. N., *et al*. 2015)

Primers:

Primers used in this study, shown in the 5'-to-3' orientation:

CG4096CRISPRsenseNOPAM: CTTCGGTGGCGTACGTCCGCTTTA

CG4096CRISPRantiNOPAM: AAACTAAAGCGGACGTACGCCACC

ScCRISPRsense: CTTCCCGGTTTTATGGATCCGGCG

ScCRISRPanti: AAACCGCCGGATCCATAAAACCGG

FP.CG4096.PCR: AAACTAAAGCGGACGTACGCCACC

RP.CG4096.PCR: GGTGGCGCTCCACCACCAG

W.CRISPRsenseNOPAM: CTTCGGCACAATACGACATCTTT

W.CRISPRantiNOPAM: AAACAAAGATGTCCATATTGTGCC

Injections:

CG4096^{EPgy2} embryos were collected based on the protocol from Kiehart *et al*. 2000. The injection mixture was prepared with 10X injection buffer (1mM Sodium Phosphate Buffer pH 6.8, 50mM KCl), green food dye, nuclease-free water and the following plasmids: Actin5C-Gal4 (200 ng/µL), pU6-GuideRNA.CG4096 (150 ng/µL), pU6-GuideRNA.w (150 ng/µL), and pUAST-Cas9-SV40 (300 ng/µL).

Immunohistochemistry:

Late third instar wing discs were stained for actin using Rhodamine phalloidin (ThermoFisher Scientific) using methods describe in Copppey *et al*. (2008). Rhodamine phalloidin was used at 1:1000 dilution and samples were mounted in ProLong® Gold Antifade Mountant with DAPI (ThermoFisher Scientific).

Results and Discussion

RNAseq analysis of inducible Ras^{V12} GSR cells identifies known and candidate Ras pathway genes

Based on the success of previous reverse genetic screens in our lab that generated new Egfr regulators like *CG4096*, I constructed a similar experimental methodology (Figure 3) to identify new Ras pathway interactors. RNAseq was performed on the GSR cells in order to identify genes induced in response to *Ras^{V12}* expression. Comparative RNAseq data analysis found a total of 363 gene transcripts that were upregulated by two-fold or greater when *Ras^{V12}* expression was induced. I selected the top 98 upregulated genes for bioinformatics analysis, and complete GO information of the 98 genes is provided in Appendix 1. Expression profiles of a subset of genes selected for functional analyses can be seen in Figure 2.

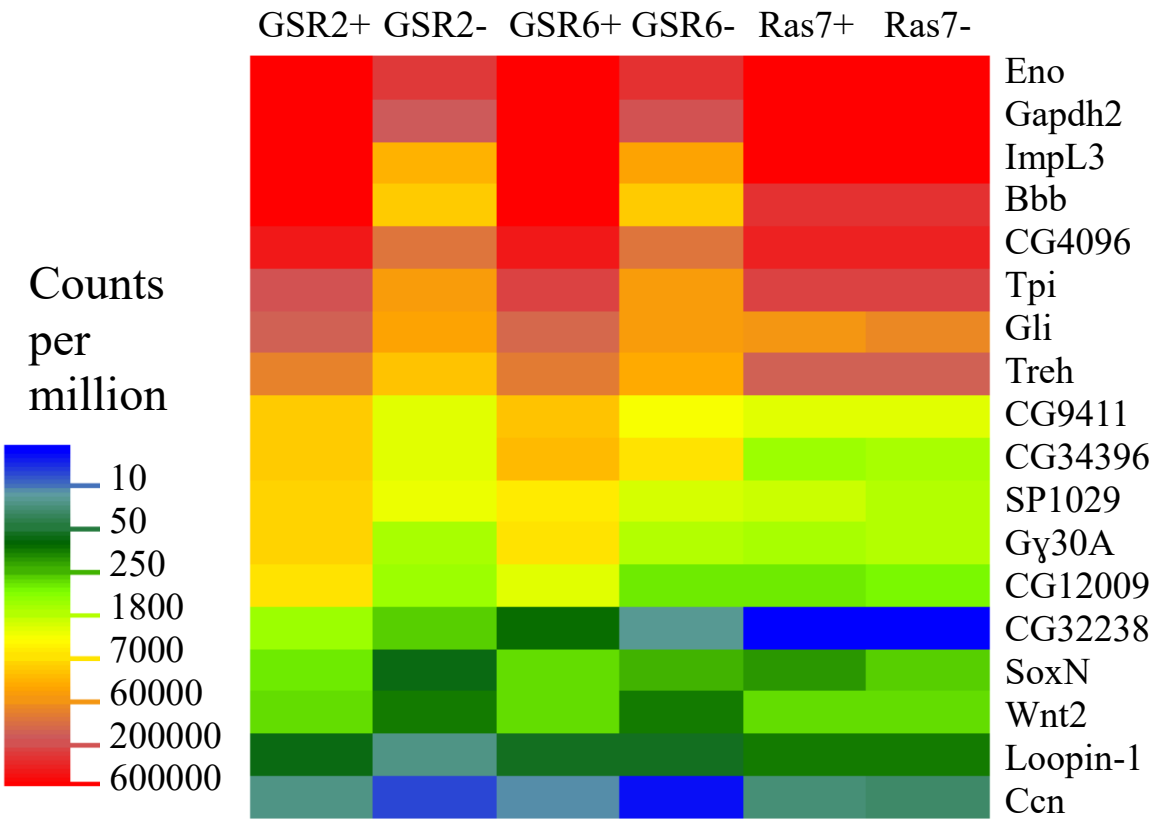

Figure 2: Heat map of a subset of candidate genes upregulated in GSR+ cells

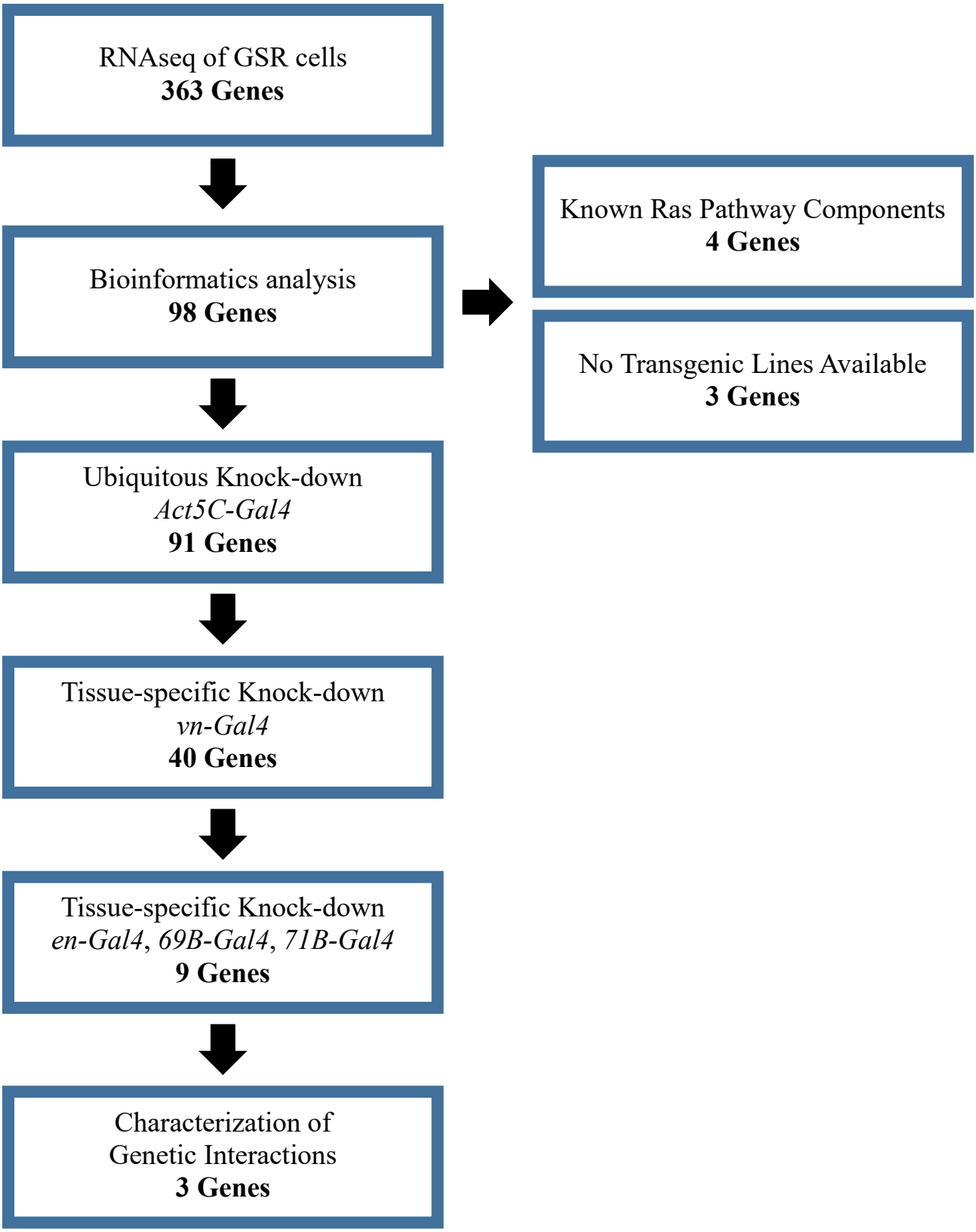

Figure 3: Experimental flow chart for functional analysis of candidate genes

Functional analysis of candidate genes using ubiquitous RNAi-induced knock-down

Of the 98 most upregulated genes, three genes are known components of the Ras pathway: *Ras85D*, *branchless* (Gabay, L. *et al.* 1997), and *CG4096* (Butchar *et al.* 2012). One gene, *wingless*, has been previously shown to interact with the Ras signaling pathway (Carmena, A. *et al*. 2006). Three genes lacked available transgenic lines (*CG4914*, *CG34194*, *CG9165*). I therefore conducted a functional analysis of the remaining 91 genes using RNAi. RNAi transgenes were ubiquitously expressed using *Act5C-Gal4*. Silencing of 40 genes affected viability – lethality (38), low viability (1) – or generated a held out wings phenotype (1) (Figure 4). Crosses were conducted at 29°C to enhance *Gal4* activity in order to increase RNAi effects (Dietzl G. *et al.* 2007). Appendix 2 lists results of all the crosses conducted for both ubiquitous and tissue-specific knock-downs of the candidate genes.

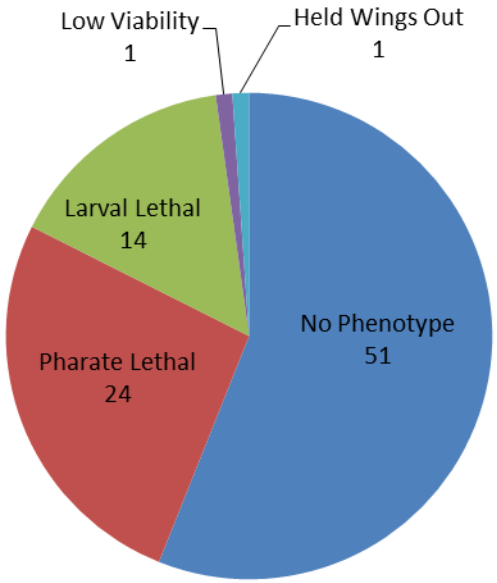

Figure 4: A breakdown of the RNAi phenotypes seen from *Act5C-Gal4*

Recently, it has been shown that approximately 25% of transgenic lines from the VDRC KK RNAi collection cause false-positive enhancement of the gene *tiptop* (*tio*) due to an insertion into the *tio* 5' UTR (Vissers *et al*. 2016; Green *et al*. 2014). *tio* is a transcription factor in Hippo pathway, which controls tissue growth (Vissers *et. al.* 2016). This enhancement results in in pupal lethality when broadly expressed and in wing phenotypes when expressed by wing-specific *Gal4* lines (Vissers *et al*. 2016; Green *et al*. 2014). I found that 6/33 (18%) of the KK lines used in this study were indeed affected by this false positive enhancement, showing pupal lethality in *Act5C-Gal4*, small uninflated wings in *69B-Gal4*, and smaller wings in *71B-Gal4*. With *71B-Gal4*, I could still screen for venation defects in these candidates, however none were observed with any of these candidates.

Tissue-specific knock-down reveals three candidate genes involved in wing development

To further refine the role of the 39 genes for which ubiquitous knock-down was lethal, I conducted tissue-specific knock-down mediated by several Gal4 lines. First, I used *vn-Gal4* to inhibit gene expression in the same expression pattern as *vn*, an Egfr ligand. The *vn-Gal4* driver contains Gal4 inserted into the 2nd exon of the vn gene, creating a loss of function allele of vn (Austin *et al*. 2015). *vn-Gal4* provides a sensitized genetic background I took advantage of to identify genes in the Egfr/Ras pathway. RNAi depletion driven by *vn-Gal4* caused phenotypes in 9 of 39 genes (Table 1). A compilation of all crosses is shown in Appendix 2. I further selected candidates that showed wing-vein phenotypes with other Gal4 drivers as well (*en-Gal4*, *69B-Gal4*, and *71B-Gal4*). We chose Gal4 drivers for their property to silence candidate genes in various compartments of the adult wing and at different times of wing development (Figure 5). Crosses were first carried out at 29°C for the strongest effect, and were repeated at 17°C and 25°C when knock-down was lethal at 29°C.

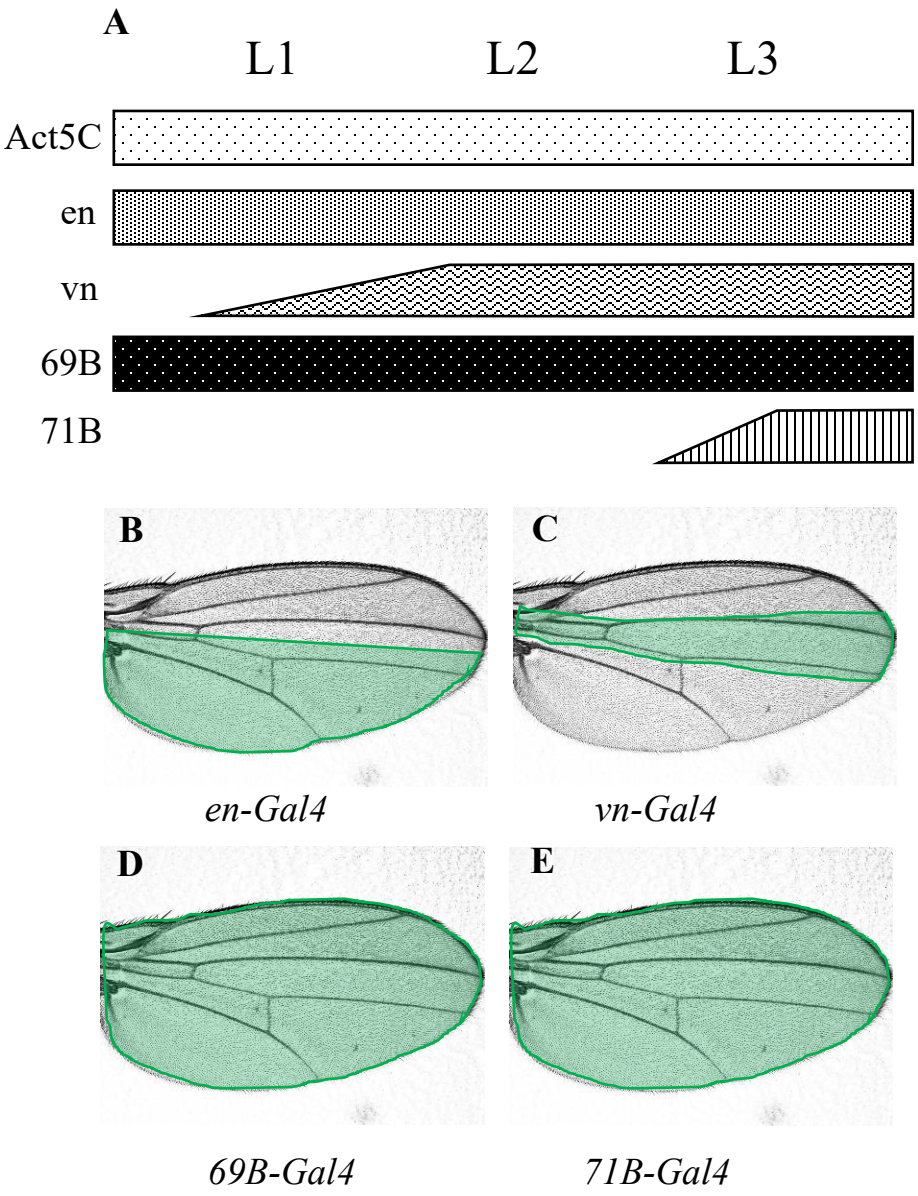

Figure 5: (A) Time-specific expression pattern in the wing disc of the Gal4 lines used, with larval stage indicated above the chart (B-E) Expression pattern of the Gal4 drivers shown in the adult wing

Based on wing phenotypes with *vn-Gal4* and other Gal4 lines, we chose 3 genes for further investigation (Figure 6). Knock-down of *Gγ30A* caused lethality when directed by *vn-Gal4* and a consistent extra-vein phenotype with the other three Gal4 drivers. Several genes showed a loss of the anterior cross vein with *vn-Gal4*, which is sensitive to Egfr signaling (Clifford and Schupbach 1989 and Schnepp *et al.* 1996). I focused only on *CG12009* and *CG31689* for further analysis as these genes show vein loss with *en-Gal4* as well.

Table 1: Genes showing phenotypes with vn-Gal4

Gene	Human Ortholog	Molecular Function	RNAi Phenotype Act5C-Gal4	RNAi Phenotype vn-Gal4	RNAi Phenotype with Other Gal4 Lines
Gγ30A	guanine nucleotide binding protein gamma 13	Protein heterodimerization activity, signal transducer activity	Lethal	Lethal	Extra vein: en-Gal4, 69B-Gal4, 71B-Gal4
SP1029	Alanyl aminopeptidase	aminopeptidase activity, metallopeptidase activity, zinc ion binding	Lethal	Lethal	Extra vein: en-Gal4
CG31689	ATP binding cassette subfamily G member 1	ATPase activity, coupled to transmembrane movement of substances	Lethal	Loss of vein	Loss of vein: en-Gal4
CG8483	GLI pathogenesis related 1	unknown	Lethal	Loss of vein	Loss of vein: en-Gal4
CG34396	potassium two pore domain channel subfamily K member 18	open rectifier potassium channel activity	Lethal	Loss of vein	None
ccn	connective tissue growth factor	growth factor activity	Lethal	Loss of vein	Loss of vein: en-Gal4
CG12009	Fibrous sheath CABYR binding protein	chitin binding	Lethal	Loss of vein	Loss of vein: en-Gal4
CG32512	transmembrane protein 205	unknown	Lethal	Lethal	Lethal: 69B-Gal4, 71B-Gal4
loopin-1	leucine aminopeptidase 3	aminopeptidase activity, manganese ion binding, metalloexopeptidase activity	Lethal	Lethal	None

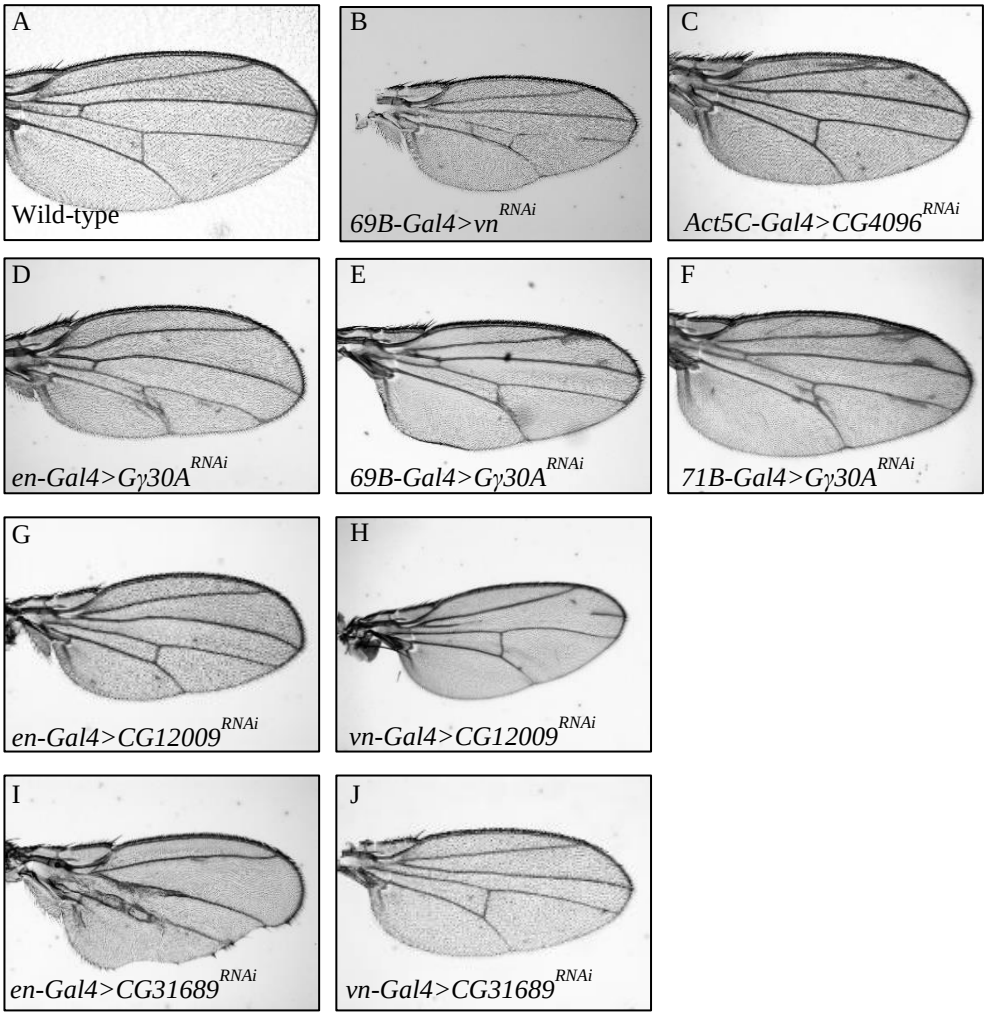

Figure 6: Wing phenotypes caused by RNAi in restricted domains
(A) Wild-type wing (B) Control: *vn* is a known positive regulator of Ras signaling and shows wing vein loss when knocked-down (C) Control: *CG4096* is a known negative regulator of Ras signaling and shows extra wing veins when knocked-down (D-F) Knock-down of *Gγ30A* causes extra vein phenotypes (G-H) Knockdown of *CG12009* causes loss of vein phenotypes (I-J) Knock-down of *CG31689* causes loss of vein phenotypes

Gγ30A: *Gγ30A* encodes a G protein gamma subunit of unknown function. Gγ30A has been shown to dimerize with Gβ76C in the cytoplasm and to be involved in the *Drosophila* visual transduction in the compound eye (Schulz *et al*. 1999). RNAi silencing of *Gγ30A* resulted in lethality with *vn-Gal4* and in extra vein phenotypes that were indistinguishable with *en-Gal4*, *69B-Gal4*, and *71B-*

Gal4 (Figure 6 D-D"). These extra vein patterns are also similar to those seen in $Egfr^{Elp}$, which is a hypermorphic allele of *Egfr* that causes extra vein phenotypes. The observed extra vein phenotypes suggest that *Gγ30A* may be a negative regulator of Ras signaling. The human ortholog of *Gγ30A*, guanine nucleotide binding protein gamma 13 (*GNG13*) dimerizes with Gβ1 and Gβ3 and activates two phospholipases (PLCβ1 and PLCβ3) (Poon *et al*. 2009). PLCβ1 has been shown to activate protein kinase C (PKC) and activate raf through a p21/ras-independent mechanism (Van Biesen *et al*. 1996). Restoration of PLCβ3 was shown to inhibit growth rate and neoplasticity in neuroendocrine tumorigenesis (Stalberg *et al*. 1999). Thus, it would be important to conduct further experiments to understand the role of *Gγ30A* in *Drosophila*.

CG12009: *CG12009* is an uncharacterized gene containing a chitin binding domain and is predicted to localize in the extracellular region. Little is known about its human ortholog, *FSCB* (Fibrous Sheath CABYR binding protein). *FSCB* has been shown to be phosphorylated by protein kinase A and is involved in fibrous sheath biogenesis (Li *et al*. 2007). In flies, knock-down of *CG12009* causes loss of the anterior cross vein (ACV) and parts of the 3rd longitudinal vein when directed by *vn-Gal4* (Figure 6 E') and loss of the ACV when directed by *en-Gal4* (Figure 6 E). These loss of vein phenotypes suggests that *CG12009* may be a positive regulator in Ras signaling. Ongoing analyses aim to test this hypothesis.

CG31689: *CG31689* is another uncharacterized gene containing domains predicted to be involved in ATPase activity coupled to transmembrane movement of substances. Its human ortholog *ABCG1* (ATP-binding cassette transporter G1) is a member of the ABC transporter family and regulates cellular cholesterol homeostasis by effluxion of excess cholesterol from cells to high-density lipoportein (HDL) particles for elimination of cholesterol from the body (Kennedy *et al*. 2005 and Wang *et al*. 2004). In my RNAi screen in *Drosophila*, *CG31689* depletion resulted in

the loss of the ACV with *vn-Gal4* and a more severe vein and wing size losses with *en-Gal4* (Figure 6 F-F'). These loss of vein phenotypes suggest that *CG31689* plays a positive role in vein patterning and potentially in Ras signaling. Reports point at a role of *ABCG1* in several types of cancers (El Roz *et al*. 2012 and Sag *et al*. 2015). Recently, loss of *ABCG1* in mice was shown to impair tumor growth and increases animal survival through the modulation of macrophage survival within the tumor microenvironment (Sag *et al*. 2015). Further analysis on how *ABCG1* and cholesterol metabolism affect tumor immunity could lead to new therapeutic approaches.

Further interaction analysis to link candidates to the Ras pathway

While it is evident that *Gγ30A*, *CG12009*, and *CG31689* are involved in wing vein patterning, further analysis is needed to link these genes to the Ras pathway; a model of the predicted interactions between the candidates and Ras is shown in Figure 7. I am proposing some experiments that will characterize the genetic interactions between these genes and the Ras pathway.

First, in vivo genetic interactions will be determined by testing the knock-down of the candidate gene in two different mutant backgrounds in flies: $Egfr^{Elp}$ (a hypermorphic mutant of *Egfr*) and $Ras85D^{e1B}$ (a null mutant of Ras). Our expectation is that in the $Egfr^{Elp}$ background will enhance the extra vein phenotype of a negative regulator (*Gγ30A*) and eliminate the loss of vein phenotype of a positive regulator (*CG12009* or *CG31689*). If genetic interactions exist between the candidate and the Ras, the heterozygous $Ras85D^{e1B}$ background would enhance the loss of vein phenotype of a positive regulator or eliminate the extra vein phenotype of a negative regulator.

A second approach to further characterization of the candidates will use RNAi-induced knock-down in cell culture. Wts cells established in the lab are particularly suited to study Egfr/Ras

signaling components: these cells are epithelial in nature, and compared to commonly used *Dosophila* cell lines (S2 and Kc), Wts cells express the core Egfr pathway genes at much higher levels (Figure 8). This provides a good system to test alterations in Egfr/Ras signaling. After conducting the knock-downs, I will test for changes in dp-ERK levels by immunoblot analysis. ERK is phosphorylated when Ras is activated (Figure 9), so if levels of dp-ERK change after knock-down of a candidate gene, that gene is a component of the Ras signaling pathway.

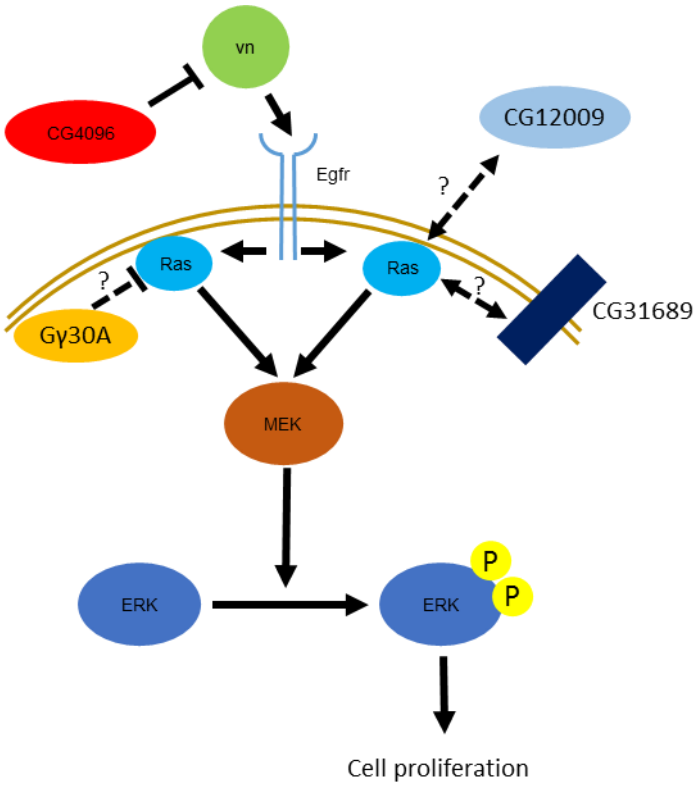

Figure 7: A simplified model of the Egfr/Ras pathway including the potential roles of candidate genes *Gγ30A*, *CG12009*, and *CG31689*

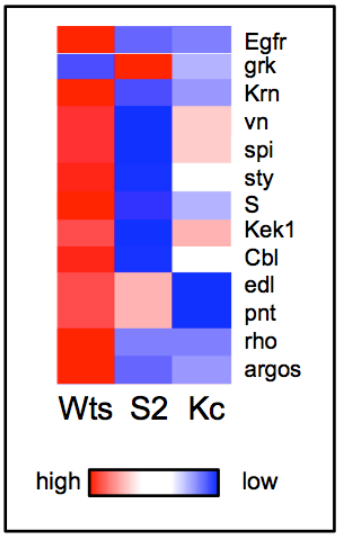

Figure 8: Expression levels of EGFR pathway genes in Wts cells compared to other Drosophila cell lines determined by microarray analysis. (Simcox Lab, unpublished)

Literature Cited

1. Austin, C. L., Manivannan, S. N., and A. Simcox, 2014. TGF-α ligands can substitute for the neuregulin Vein in *Drosophila* development. Dev. 141:4110-4114.
2. Blair, S. S., 2007 Wing vein patterning in Drosophila and the analysis of intercellular signaling. Annu. Rev. Cell Dev. Biol. 23: 293-319.
3. Carmena, A., Speicher, S., and M. Baylies, 2006. The PDZ protein canoe/AF-6 links Ras-MAPK, Notch and wingless/Wnt signaling pathways by directly interacting with Ras, Notch, and disheveled. PLoS One. 1:e66
4. Coppey, M., A. N. Boettiger, A. M. Berezhkovskii, and S. Y. Shvartsman, 2008. Nuclear trapping shapes the terminal gradient in the Drosophila embryo. Curr. Biol. 18: 915-919.
5. Dietzl, G., Chen, D., Schnorrer, F., Su, K.C., Barinova, Y. *et al.*, 2007. A genome-wide transgenic RNAi library for conditional gene inactivation in Drosophila. Nature. 448(7150): 151-6.
6. Downward, J. Targeting RAS signaling pathways in cancer therapy. Nat Rev Cancer, 2003. 3(1): 11-22.
7. El Roz, A., Bard, J., Huvelin, J., and H. Nazih, 2012 LXR Agonists and ABCG1-dependent Cholesterol Efflux in MCF-7 Breast Cancer Cells: Relation to Proliferation and Apoptosis. Anticanc. Res. 32(7), 3007-3013.
8. Gabay, L., Seger, R., and B. Shilo, 1997. MAP kinase in situ activation atlas during *Drosophila* embryogenesis. Dev. 124, 3535-3541.
9. Gratz, S.J., Rubinstein, C.D., Harrison, M.M., Wildonger, J., and O'Connor-Giles, K.M. 2015. CRISPR-Cas9 genome editing in *Drosophila*. Curr. Protoc. Mol. Biol. 111:31.2.1-31.2.20.
10. Green, E. W., Fedele, G., Giogini, F., and C.P. Kyriacou, 2014. A *Drosophila* RNAi collection is subject to dominant phenotypic effects. *Nat. Meth*. 11(3):222-3.
11. Gysin, S.,Salt, M., Young, A., and F. McCormick, 2011. Therapeutic strategies for targeting ras proteins. Genes Cancer 2(3): 359-72.
12. Han M. and P.W. Sternberg, 1990. *let-60*, a gene that specifies cell fates during *C. elegans* vulval induction, encodes a *ras* protein. Cell 63(5): 921-931.
13. Jacobsen, T.L., Cain, D., Paul, L., Justiniano, S., Alli, A. *et al*. 2006, Functional Analysis of Genes Differentially Expressed in the Drosophila Wing Disc: Role of Transcripts Enriched in the Wing Region. Genetics 174(4): 1973–1982.
14. Jia, D., Soylemez, M., Calvin, G., Bornman, R., Bryant, J. *et al*. 2015. A large-scale in vivo RNAi screen to identify genes involved in Notch-mediated follicle cell differentiation and cell cycle switches. Sci Rep. 5: 12328.
15. Kennedy, M.A., Barrera, G.C., Nakamura, K., Baldan, A., Tarr, P. *et al*. 2005. ABCG1 has a critical role in mediating cholesterol efflux to HDL and preventing cellular lipid accumulation. Cell Metab. 1(2): 121-31.

16. Kiehart, D. P., Crawford, J.M., and R.A. Montague, 2007. Collection, Dechorionation, and Preparation of *Drosophila* Embryos for Quantitative Microinjection. Cold Spring Harb Protoc doi:10.1101/pdb.prot4717.
17. Lee, M. and V. Vasioukhin, 2008. Cell polarity and cancer – cell and tissue polarity as a non-canonical tumor suppressor. Journal of Cell Sci. 121: 1141-50.
18. Li, P., Mao, X., Ren, Y. and Liu P, 2015. Epithelial Cell Polarity Determinant CRB3 in Cancer Development. Int J Biol Sci 11(1):31-37.
19. Li, Y.F., He, W., Jha, K.N., Klotz, K., Kim, Y.H. *et al*. 2007 FSCB, a novel protein kinase A-phosphorylated calcium-binding protein, is a CABYR-binding partner involved in late steps of fibrous sheath biogenesis. J. Biol. Chem. 282(47): 34104-19.
20. Luo, J., Zuo, J., Wu, J., Wan, P., Kang, D. *et al*. 2015. *In viv* RNAi screen identifies candidate signaling genes required for collective cell migration in *Drosophila* ovary. Sci China Life Sci. 58 (4): 379-389.
21. Manivannan, S.N., Jacobsen, T.L., Lyon, P., Selvaraj, B., Halpin, P., and A. Simcox, 2015. Targeted Integration of Single-Copy Transgenes in *Drosophila melanogaster* Tissue-Culture Cells Using Recombination-Mediated Cassette Exchange. Genetics 201: 1319-1328.
22. Nicholson, L., Singh, G.K., Osterwalder, T., Roman, G.W., Davis, R.L. *et al*. 2008. Spatial and temporal control of gene expression in *Drosophila* using the inducible GeneSwitch GAL4 system: screen for larval nervous system drivers. Genetics 178(1): 215-234.
23. Osterwalder, T., K.S. Yoon, B.H. White, and H. Keshishian, 2001. A conditional tissue-specific transgene expression system using inducible GAL4. Proc Natl Acad Sci U S A, 98(22): p. 12596-601.
24. Poon, S.W.L., Chan A.S.L., and Y.H. Wong. 2009. Gβ3 forms distinct dimers with specific Gγ subunits and preferentially activates the β3 isoform of phospholipase C. Cell. Sig. 21(5): 737-744.
25. Porter, S., Span, P.N., Sweep, F.C., Tjan-Heijnen, V.C., Pennington, C.J. *et al*. 2006. ADAMTS8 and ADAMTS15 expression predicts survival in human breast carcinoma. Int J Cancer 118: 1241-7.
26. Richter, C., Chang, J.T., and P.C. Fineran, 2012. Function and Regulation of Clustered Regularly Interspace Short Palindromic Repeats (CRISPR)/CRISPR Associated (Cas) Systems. *Viruses* 4, 2291-311.
27. Roch, F., Jimenez, G., and J. Casanova, 2002. EGFR signaling inhibits Capicua-dependent repression during specification of *Drosophila* wing veins. Dev. 129: 993-1002.
28. Sag, D., Cekic, C., Wu, R., Liden, J., and C. C. Hedrick, 2015. The cholesterol transporter ABCG1 links cholesterol homeostasis and tumour immunity. Nat. Commun. 6:6354

29. Schulz, S., Huber, A., Schwab, K., and R. Paulsen, 1999. A novel Gγ isolated from *Drosophila* constitutes a visual Gγ protein subunit of the fly compound eye. J. Biol. Chem. 274(53): 37605-10.
30. Simon, M.A., Bowtell, D.D., Dodson, G.S., Laverty, T.R. and G.M. Rubin, 1991. Ras1 and a putative guanine nucleotide exchange factor perform crucial steps in signaling by the sevenless protein tyrosine kinase. Cell 67(4): p. 701-16.
31. Stalberg, P., Wang, S., Larsson, C., Weber, G., Oberg, K. *et al*. 1999. Suppresion of the neoplastic phenotype by transfection of phospholipase C β3 to neuroendocrine tumor cells. FEBS Letters, 450, doi:10.1016/S0014-5793(99)00457-3
32. Van Biesen, T., Luttrell, L.M., Hawes, B.E., and R.J. Lefkowitz, 1996. Mitogenic Signaling via G Protein-Coupled Receptors. Edocr. Rev. 17: 698-714.
33. Vissers, J. H. A. Manning, S.A., Kulkarni, A., and K.F. Harvey, 2016. A *Drosophila* RNAi library modulates Hippo pathway-dependent tissue growth. Nat. Commun. 7:10368
34. Wagstaff, L., Kelwick, R., Decock, J. and D.R. Edwards, 2011. The roles of ADAMTS metalloproteinases in tumorigenesis and metastasis. Front Biosci 16, 1861-72.
35. Wang, N., Lan, D., Chen, W., Matsuura, F. and A.R. Tall, 2004. ATP-binding cassette transporters G1 and G4 mediate cellular cholesterol efflux to high-density lipoproteins. Proc. Nat. Acad. Sci. 101: 9774-79.
36. Zhao B., Wei, X., Li, W., Udan, R.S., Yang, Q. *et al*. 2007. Inactivation of YAP oncoprotein by the Hippo pathway is involved in cell contact inhibition and tissue growth control. Genes Dev. 1;21(21):2747-61.

Appendix 1:

GO classification of upregulated Ras-responsive genes

Gene Name	Human Ortholog	Molecular Function	Biological Process
Major heat shock 70 kDa protein Bbb	heat shock 70kDa protein 1A; heat shock 70kDa protein 1B	heat shock-mediated polytene chromosome puffling, response to heat, response to hyperoxia	protein folding, protein complex assembly, response to stress
Ecdysone-inducible gene L3	lactate dehydrogenase A-like 6A	L-lactate dehydrogenase activity	glycolysis, oxidation-reduction process, cellular carbohydrate metabolic process, tricarboxylic acid cycle
branchless	fibroblast growth factor 16	fibroblast growth factor receptor binding	activation of MAPK activity
CG4914	protease, serine, 33	serine-type endopeptidase activity	proteolysis
CG15731	loricrin	Unknown	Unknown
CG9416	endoplasmic reticulum metallopeptidase 1	peptidase activity	proteolysis
CG14968	family with sequence similarity 43, member B	protein binding, receptor binding	apoptotic process, immune system process
CG8483	C-type lectin domain family 18, member A	Unknown	Unknown
UPF0670 protein	chromosome 8 open reading frame 55	Unknown	Unknown
Ecdysone-inducible gene L2	cell adhesion molecule 2	insulin-like growth factor binding	determination of adult lifespan, negative and positive regulation of insulin receptor signaling pathway,
CG8277	eukaryotic translation initiation factor 4E family member 1B	eukaryotic initiation factor 4G binding, protein binding, RNA 7-methylguanosine cap binding, translation initiation factor activity	autophagic cell death, salivary gland cell autophagic cell death, translational initiation

quail	villin-like	actin binding, calcium ion binding	actin filament organization, imaginal disc-derived wing hair organization, ovarian nurse cell to oocyte transport
kin of irre	nephrosis 1, congenital, Finnish type (nephrin)	Unknown	compound eye morphogenesis, garland nephrocyte differentiation, homophilic and heterophilic cell adhesion
Probable mitochondrial import inner membrane translocase subunit Tim17 3	translocase of inner mitochondrial membrane 17 homolog A (yeast)	Unknown	cellular process, mitochondrial and protein transport
G protein gamma30A	guanine nucleotide binding protein (G protein), gamma 13	protein heterodimerization activity, GTPase activity, signal transducer activity	cellular response to carbon dioxide, phototransduction
Ras oncogene at 85D	neuroblastoma RAS viral (v-ras) oncogene homolog	GTPase activity, protein binding	border follicle cell migration, cell proliferation, cell fate determination
SoxNeuro	sex determining region Y	chromatin DNA binding, protein binding, RNA polymerase II distal enhancer sequence-specific DNA binding transcription factor activity	axon guidance, (central) nervous system development
CG13838	chromosome 9 open reading frame 16	unknown	unknown
CG34194	chromosome 14 open reading frame 147	unknown	unknown
Nidogen	nidogen 2 (osteonidogen)	calcium ion binding	cell-matrix adhesion

Probable 2-oxoglutarate dehydrogenase E1 component DHKTD1 homolog, mitochondrial	dehydrogenase E1 and transketolase domain containing 1	Unknown	Unknown
wunen-2	phosphatidic acid phosphatase type 2C	lipid phosphatase and transporter/pyrophosphatase activity	germ cell development, migration, programmed cell death, and repulsion, dephosphorylation, phospholipid metabolic process
CG7432	protease, serine 27	serine-type endopeptidase activity	proteolysis
CG9411	proline-rich protein BstNI subfamily 1; proline-rich protein BstNI subfamily 2; proline-rich protein BstNI subfamily 4	unknown	unknown
stall	ADAM metallopeptidase with thrombospondin type 1 motif, 13	metallopeptidase activity, protein binding, serine-type endopeptidase inhibitor activity, zinc ion binding	proteolysis, cell-cell adhesion and cell communication, regulation of catalytic activity, ovarian follicle development
Glyceraldehyde 3 phosphate dehydrogenase 2	glyceraldehyde-3-phosphate dehydrogenase-like 6; hypothetical protein LOC100133042; glyceraldehyde-3-phosphate dehydrogenase	catalytic activity, oxidoreductase activity	glycolysis
minidiscs	solute carrier family 7, (cationic amino acid transporter, y+ system) member 11	amino acid transmembrane transporter activity	amino acid transmembrane transport, leucine import
CG32512	transmembrane protein 205	unknown	unknown

wingless	wingless-type MMTV integration site family, member 4	receptor binding, protein binding, extracellular matrix binding	cell communication, cell differentiation, regulation of biological process, nervous system development, many cells differentiation and development (not all listed here)
CG18480	leucine rich repeat containing 33	receptor activity	immune system process, cell communication, cell-cel adhesion, visual perception
CG14309	heparanase 2	hydrolase activity, acting on glysosyl bonds	Unknown
CG31092	low density lipoprotein receptor-related protein 8, apolipoprotein e receptor	calcium ion binding, low-density lipoprotein receptor activity	neuron projection morphogenesis
CG4438	PDGFA associated protein 1; similar to PDGFA associated protein 1	Unknown	Unknown
CG10859	dynein, axonemal, intermediate chain 2	ATPase activity- coupled, motor activity, structural constituent of cytoskeleton	microtubule-based movement, cellular component morphogenesis, RNA localization
Farnesyl pyrophosphate synthase	farnesyl diphosphate synthase (farnesyl pyrophosphate synthetase, dimethylallyltranstransferase, geranyltranstransferase)	dimethylallyltranstransferase activity, geranyltranstransferase activity	wing disc development, germ cell migration, farnesyl diphosphate biosynthetic process, isoprenoid biosynthetic process
CG11153	SRY (sex determining region Y)-box 6	sequence-specific DNA binding transcription factory activity	transcription and regulation of transcription from RNA polymerase II promoter

Heparan sulfate 3-O sulfotransferase-B	heparan sulfate (glucosamine) 3-O-sulfotransferase 3A1	[heparan sulfate]-glucosamine 3-sulfotransferase 1 activity	morphogenesis of chaeta, compound eye, and imaginal disc-derived leg and wing (more biological processes not listed here)
CG34392	Rap guanine nucleotide exchange factor (GEF) 4	cAMP-dependent protein kinase regulator activity, Rap guanyl-nucleotide exchange factor activity, catalytic activty, small GTPase regulator activity, protein binding	regulation of Rap protein signal transduction, metabolic process, mitosis, cell communication, regulation of catalytic activity
CG31689	ATP-binding cassette, sub-family G (WHITE), member 4	ATP binding, ATPase activity, coupled to the transmembrane movement of substances, transporter activity	Unknown
tenectin	A kinase (PRKA) anchor protein 12	integrin binding	morphogenesis of imaginal disc-derived wing and imaginal disc-derived male genitalia, embryonic hindgut, and epithelial tube; regulation of tube diameter
CG12009	fibrous sheath CABYR binding protein	chitin binding	chitin metabolic process
CG11652	DPH1 homolog (S. cerevisiae)	unknown	phagocytosis, peptidyl-diphthamide biosynthetic process from peptidyl-histidine
CG34396	potassium channel, subfamily K, member 18	voltage-gated potassium channel activity	sytem process, cation transport, potassium ion transmembrane transport
pathetic	solute carrier family 36 (proton/amino acid symporter), member 3	amino acid transmembrane transporter activity	growth and growth regulation, intracellular protein and peroxisomal transport

CG16869	angiotensin I converting enzyme (peptidyl-dipeptidase A) 1	NOT metallopeptidase or peptidyl-dipeptidase activity activity	proteolysis
CG15286	potassium channel modulatory factor 1	zinc ion binding	no information found on Flybase or Panther
nuclear export factor 4	nuclear RNA export factor 1	Unknown	RNA export from nucleus
CG34107	chromosome 9 open reading frame 116	Unknown	unknown
Enolase	enolase 1, (alpha)	magnesium ion binding, catalytic activity, phosphopyruvate hydratase activity	glycolysis
CG32238	tubulin tyrosine ligase-like family, member 1	tubulin-tyrosine ligase activity	C-terminal protein-tyrosinylation, protein polyglutamylation
Probable cytochrome P450 28d1	cytochrome P450, family 3, subfamily A, polypeptide 4	electron carrier activity, heme binding, iron ion binding, oxidoreductase activity, acting on paired donors, with incorporation or reduction of molecular oxygen	oxidation-reduction process
CG34372	G protein-coupled receptor 179	G-protein coupled receptor activity	G-protein coupled receptor signaling pathway
CG18173	phosphatidylinositol glycan anchor biosynthesis, class W	transferase activity, transferring acyl groups	GPI anchor biosynthetic process
CG13320	Usher syndrome 1G (autosomal recessive)	Unknown	Unknown
no extended memory	glutaminase 2 (liver, mitochondrial)	carbon-monoxide oxygenase activity,	imaginal disc-derived wing morphogenesis, locomotory behavior, memory

CG15478	MAX binding protein	sequence-specific DNA binding transcription factor activity,	regulation of transcription from RNA polymerase II promoter
CG3777	mucin 17, cell surface associated	Uknown	proteolysis lysosomal transport intracellular protein transport
Regulator of G-protein signalling 7	regulator of G-protein signaling 6	GTPase activator activity, signal transducer activity	intracellular signal transduction, regulation of G-protein coupled receptor protein signaling pathway, termination of G-protein coupled receptor signaling pathway
Multiple inositol polyphosphate phosphatase 1	multiple inositol polyphosphate histidine phosphatase, 1	acid phosphatase activity, phosphoprotein phosphatase activity	Uknown
centaurin gamma 1A	ArfGAP with GTPase domain, ankyrin repeat and PH domain 4; ArfGAP with GTPase domain, ankyrin repeat and PH domain 6	zinc ion binding, GTP binding, ARF GTPase activator activity	small GTPase mediated signal transduction, regulation of ARF GTPase activity
CG6330	uridine phosphorylase 2	uridine phosphorylase activity	gravitaxis, nucleoside metabolic process, nucleotide catabolic process
CG16957	progesterone receptor membrane component 1	heme binding	
CG4415	NAC alpha domain containing	unfolded protein binding	protein targeting
CG32183	WNT1 inducible signaling pathway protein 3	growth factor activity	neurogenesis
yolkless	epidermal growth factor (beta-urogastrone)	calcium ion binding, vitellogenin receptor activity	vitellogenesis, oogenesis

CG5002	solute carrier family 26, member 11	transporter activity, high affinity sulfate transmembrane transporter activity	sulfate transport
CG11546	GIPC PDZ domain containing family, member 3	G-protein alpha-subunit binding	locomotion involved in locomotory behavior, establishment of planar polarity, determination of adult lifespan
Triose phosphate isomerase	TPI1 pseudogene; triosephosphate isomerase 1	triose-phosphate isomerase activity	response to mechanical stimulus, neurological system process, determination of adult lifespan
lethal (3) 02640	hydroxymethylbilane synthase	hydroxymethylbilane synthase activity	tetrapyrrole biosynthetic process, peptidyl-pyrromethane cofactor linkage
CG4096	ADAM metallopeptidase with thrombospondin type 1 motif, 10	zinc ion binding, metalloendopeptidase activity	negative regulation of epidermal growth factor receptor signaling pathway, proteolysis
Netrin-B	laminin, alpha 4	unknown	axon guidance, dendrite guidance, glial cell migration,salivary gland boundary specific
CG34420	dipeptidase 1 (renal)	dipeptidase activity	proteolysis
CG15556	G protein-coupled receptor 113	G-protein coupled receptor activity	G-protein coupled receptor signaling pathway
Wnt oncogene analog 2	wingless-type MMTV integration site family, member 3A	frizzled binding, receptor binding	open tracheal system development, muscle organ development, axon extension, negative regulation of transcription from RNA polymerase II promoter, Wnt receptor signaling pathway

CG10996	galactose mutarotase (aldose 1-epimerase)	aldose 1-epimerase activity, carbohydrate binding	hexose metabolic process
Malic enzyme	malic enzyme 1, NADP(+)-dependent, cytosolic	malate dehydrogenase (oxaloacetate-decarboxylating) (NADP+) activity	sleep, regulation of cell death, determination of adult lifespan
Glyceraldehyde 3 phosphate dehydrogenase 1	glyceraldehyde-3-phosphate dehydrogenase, spermatogenic	glyceraldehyde-3-phosphate dehydrogenase (NAD+) (phosphorylating) activity, NAD binding, NADP binding	glycolysis, oxidation-reduction process
CG4750	leucine aminopeptidase 3	metalloexopeptidase activity, manganese ion binding, metalloexopeptidase activity	proteolysis
CG9413	solute carrier family 7 (cationic amino acid transporter, y+ system), member 9	amino acid transmembrane transporter activity	amino acid transmembrane transport
cueball	slit homolog 3 (Drosophila)	Wnt-protein binding, Wnt-activated receptor activity,low-density lipoprotein receptor activity	primary spermatocyte growth
CG15142	cyclin-dependent kinase 2 associated protein 1	kinase activity nucleic acid binding protein binding kinase inhibitor activity kinase regulator activity	DNA replication cellular protein modification process cell cycle cell communication regulation of catalytic activity

Fat body protein 2	hydroxyprostaglandin dehydrogenase 15-(NAD)	alcohol dehydrogenase (NAD) activity, nutrient reservoir activity	oxidation-reduction process
Trehalase	trehalase (brush-border membrane glycoprotein)	trehalase activity, alpha,alpha-trehalase activity	trehalose metabolic process
CG5955	short chain dehydrogenase/reductase family 42E, member 1	coenzyme binding, UDP-glucose 4-epimerase activity	cellular metabolic process
Sarcoglycan alpha	sarcoglycan, epsilon	calcium ion binding, structural constituent of muscle	unknown
CG34380	neuropilin 2	receptor signaling protein tyrosine kinase activity	cell adhesion, signal transduction
asparagine synthetase	asparagine synthetase	asparagine synthase (glutamine-hydrolyzing) activity	asparagine biosynthetic process
CG9847	FK506 binding protein 11, 19 kDa	calcium ion binding, FK506 binding, peptidyl-prolyl cis-trans isomerase activity	regulation of Notch signaling pathway, muscle cell cellular homeostasis, imaginal disc-derived wing margin morphogenesis, imaginal disc development, chaeta development
CG18599	intestine-specific homeobox	sequence-specific DNA binding transcription factor activity, sequence-specific DNA binding	regulation of transcription, DNA-dependent
Cytochrome c proximal	cytochrome c, somatic	electron carrier activity	oxidative phosphorylation
CG31454	transmembrane protein 135	unknown	unknown

SP1029	alanyl (membrane) aminopeptidase	zinc ion binding, metallopeptidase activity, aminopeptidase activity	lateral inhibition, proteolysis
Gliotactin	butyrylcholinesterase	carboxylesterase activity	synaptic target recognition, border follicle cell migration,cell adhesion involved in heart morphogenesis,establishment of blood-nerve barrier,female meiosis chromosome segregation, maintenance of imaginal disc-derived wing hair orientation, regulation of tube size, open tracheal system,
CG5665	lipase, member H	lipase activity	lipid catabolic processes
CG9485	amylo-1, 6-glucosidase, 4-alpha-glucanotransferase	4-alpha-glucanotransferase activity, amylo-alpha-1,6-glucosidase activity	glycogen catabolic process, glycogen biosynthetic process
Putative glycogen [starch] synthase	glycogen synthase 1 (muscle)	glycogen (starch) synthase activity	glycogen biosynthetic process
CG30281	fibrinogen gamma chain	receptor binding	cell communication cell-matrix adhesion cell-cell adhesion
CG6658	UDP glucuronosyltransferase 2 family, polypeptide B15	glucuronosyltransferase activity	metabolic process

Appendix 2:

RNAi analysis of candidate genes

Table A2-1: Transgenic RNAi stocks for genes with no *Act5C-Gal4* phenotype

Gene:	Stock#:
Netrin-B	BL25861, BL34698
CG11153	BL26220
CG18480	BL28529
CG9108	BL28574
CG34392	BL29217
CG31092	BL31150
yolkless	BL31152
wunen-2	BL32382, BL32423
Sarcoglycan alpha	BL34027
CG9485	BL34333
CG4415	BL35613
CG5665	BL35717
asparagine synthetase	BL35739
cueball	BL36875
Malic enzyme	BL38256, BL41652
quail	BL41856
CG13838	BL42898
CG1544	BL43310
Fbp2	BL44052, BL50545
CG34380	BL44089
CG15556	BL44574
CG16869	BL50691
CG34372	BL51472
CG9413	BL51791
CG13320	BL51829
CanA-14F	V109858

Gene:	Stock#:
CG34420	BL53932
CG11546	BL53349
CG10833	BL53892
CG31092	BL54461
CG5002	BL55359
ImpL2	BL55855
CG4666	BL55939
CG9416	V106330
Tim17a1	V101139
CG15731	V30244, V30246
Nidogen	V109625
CG7432	V31091
CG4438	V105175
CG10859	V27322
CG12389	V104362
CG7890	V110601
tenectin	V42326
CG15286	V106518
CG3777	V109678
CG10996	V104158
CG9847	V12863, V12864, V39071
CG31454	V5811
CG6904	V35136,V35137
CG30281	V108551
CG6658	V104262

Table A2-2: Transgenic RNAi Stock and cross data for genes with *Act5C-Gal4* phenotypes

Gene:	Stock #	Act5C-Gal4	En-Gal4	69B-Gal4	71B-Gal4	Vn-Gal4
G protein gamma30a	BL 25932	Pharate Lethal	No Phenotype	No Phenotype	No Phenotype	No Phenotype
	BL 34484	Larval Lethal	29°C – Larval Lethal	29°C – Larval Lethal	29°C – Pharate Lethal	29°C – Larval Lethal
			25°C – Larval Lethal	25°C – Larval Lethal	25°C – 1/3 have extra veins between L2 + L3, below L4 and on PCV. Also pharate lethal	25°C – Pharate Lethal
			17°C – Extra veins on PCV and L5	17°C – 2/2 extra wing veins on L2, L3, and PCV; pupal lethal	17°C – 23/43 have extra veins between L2 + L3 and on PCV	17°C – Pharate Lethal
SoxNeuro	BL25996	Larval Lethal	No Phenotype	No Phenotype	4/38 -wrinkled wings, 5/38 – extra vein below L3	No Phenotype
CG34396	BL26011	Pharate Lethal	29°C – Pharate Lethal 25°C - No Phenotype	No Phenotype	No Phenotype	21/49 – No ACV
Enolase	BL26300	Larval Lethal	No Phenotype	No Phenotype	No Phenotype	29°C – Lethal 25°C – No Phenotype 17°C – No Phenotype
	BL41467	Larval Lethal	No Phenotype	No Phenotype	38/86 – spots of dark pigment on wing margins, especially below L4 and L5	No Phenotype

Gapdh2	26302	Larval Lethal	29°C – Lethal 25°C – Lethal 17°C – No Phenotype	29°C – 7/28 have extra vein on PCV, some pharates 25°C – No Phenotype 17°C – No Phenotype	29°C – 3/27 have extra vein below L3, some pharate lethal 25°C –No Phenotype, some pharate lethal 17°C – No Phenotype	29°C – Lethal 25°C – Lethal 17°C – No Phenotype
tpi	26304	Pharate Lethal	No Phenotype	No Phenotype	No Phenotype	4/40 missing ACV 1/40 missing part of PCV
CG9411	28320	Pharate Lethal	No Phenotype	No Phenotype	No Phenotype	No Phenotype
Ccn	BL31715	Larval Lethal	29°C – Larval Lethal 25°C – Pharate Lethal 17°C – 28/31 have smaller wings from L4 down and no PCV	No Phenotype	No Phenotype	20/21 have no ACV and fold in wing between L3 and L4
Gliotactin	BL31869	Larval Lethal	8/10 have no ACV and wrinkled wings	29°C – 6/6 have wrinkled wings, some pharates 25°C – 62/62 have wrinkled wings 17°C – 56/56 have fold between L3 and L4	14/30 curly wings, 13/30 curly and wrinkled wing	Curly wings
ImpL3	BL33640	Low Viability	No Phenotype	No Phenotype	No Phenotype	3/47 have wrinkled wings

Hsp70Bbb	BL33916	Larval Lethal	No Phenotype	29°C – Lethal 25°C – No Phenotype	No Phenotype	No Phenotype
CG12009	BL41968	Larval Lethal	22/27 – smaller wings, no ACV	24/28 – smaller wings, region between L2 and L3 smaller	No Phenotype	13/13 – smaller wing, missing part of L3 and ACV
Trehalase	BL50585	Larval Lethal	No Phenotype	No Phenotype	No Phenotype	No Phenotype
	BL51810	Larval Lethal	No Phenotype	No Phenotype	2/49 – extra vein on PCV	No Phenotype
loopin-1	BL54012	Larval Lethal	No Phenotype	29°C – Low viability (74 CyO/5 RNAi) 25°C – No Phenotype	No Phenotype	29°C – Lethal 25°C – Lethal 17°C – Lethal
CG32238	BL54016	Larval Lethal	2/20 – extra vein below L3	No Phenotype	1/37 – blistered wing	6/41 – no ACV
SP1029	V1065785	Pharate Lethal	31/59 – extra wing vein on PCV and below L4	No Phenotype	2/98 – wrinkled wings	29°C – Lethal 25°C – Lethal 17°C – Lethal
Wnt oncogene analog 2	BL36722	Held Wings Out	No Phenotype	29°C –30/30 held wings out 25°C – 26/26 held wings out	No Phenotype	No Phenotype
	BL44271	Held Wings Out	No Phenotype	No Phenotype	No Phenotype	No Phenotype
CG15731	v30244	No Phenotype	No Phenotype	47/61 Extra vein above L2	No Phenotype	No Phenotype
	v30246	Pharate Lethal	No Phenotype	12/40 Extra vein above L2, some pharates	No Phenotype	No Phenotype

CG14968	v102790	Pharate Lethal	4/38 no ACV	19/21 - not inflated wings	No Phenotype	17/42 - pigment on wings, held wings out, 25/42 - held wings out
elF4E-5	v102173	Pharate Lethal	No Phenotype	No Phenotype	No Phenotype	No Phenotype
stall	v104737	Pharate Lethal	10/56 - dark pigment on wing 3/56 - smaller wing L3 down	Pharate lethal	No Phenotype	No Phenotype
mnd	v110217	Pharate Lethal	No Phenotype	36/71 Extra vein between L3/L4	No Phenotype	No Phenotype
CG32512	v32904	Larval Lethal	Lethal, 3/4 missing ACV	Pharate Lethal	Pharate lethal	Pharate Lethal
CG14309	v103061	Pharate Lethal	No Phenotype	Pharate lethal	No Phenotype	No Phenotype
CG31689	v102097	Pharate Lethal	11/11 - small wings, ACV loss, "serrate" like	No Phenotype	No Phenotype	26/32 - no ACV
CG11652	v103550	Pharate Lethal	20/23 - smaller wing L4 down, no ACV	No Phenotype	No Phenotype	No Phenotype
pathetic	v100519	Pharate Lethal	No Phenotype	37/54 - un-inflated wings	No Phenotype	No Phenotype
nxf4	v101011	Pharate Lethal	65/72 - smaller wing from L3 down, no ACV	Pharate lethal	No Phenotype	No Phenotype
CG34107	v109592	Pharate Lethal	25/25 - pigment on wings	29°C – Pharate lethal 17°C – 23/101 un-inflated wings	No Phenotype	35/35 wrinkled wing

CG18173	v105262	Pharate Lethal	27/51 - smaller wing L3 down 24/51 - smaller wing L3 down, no ACV	No Phenotype	No Phenotype	No Phenotype
nemy	v7909	Pharate Lethal	No Phenotype	18/83 - Extra vein above L2	No Phenotype	No Phenotype
	v40803	No Phenotype	No Phenotype	30/95 - Extra vein above L2	No Phenotype	No Phenotype
CG15478	v103025	Pharate Lethal	46/46 - pigment on wings	29°C – Pharate lethal, 2/6 adults have small, uninflated wings 17°C – No Phenotype	No Phenotype	No Phenotype
Mipps1	v101634	Larval Lethal (Male lethal)	39/39 - below L3 almost gone	No Phenotype	No Phenotype	No Phenotype
CG6330	v104776	Pharate Lethal	No Phenotype	No Phenotype	No Phenotype	No Phenotype
CG16957	v105897	Larval Lethal	No Phenotype	No Phenotype	No Phenotype	No Phenotype
CG15142	v104998	Pharate Lethal	No Phenotype	Pharate Lethal	No Phenotype	No Phenotype
CG5955	v102443	Pharate Lethal	Larval Lethal	Pharate lethal	No Phenotype	No Phenotype
CG18599	v110312	Pharate Lethal	No Phenotype	30/92 Extra vein above L2	7/35 - Extra vein above L2	No Phenotype
Cyt-c-p	v106759	Larval Lethal	Pupal Lethal	No Phenotype	No Phenotype	No Phenotype
CG8483	BL58094	Larval Lethal	27/27 smaller wing L3 down 4/27 no ACV	2/2 Low Viability, No Phenotype	No Phenotype	17/18 no ACV

*All crosses done at 29°C, unless noted

Appendix 3:

Analysis of *CG4096*, a known negative regulator of Egfr signaling

Further investigation of CG4096, a negative regulator of Egfr signaling

CG4096 expression was identified as a candidate gene upregulated in the presence of drug inducible Ras^{V12} in this study. A previous study in our lab has shown that *CG4096* is a negative regulator of Egfr signaling (upstream of Ras) and it has been empirically shown that *CG4096* is operating on the same level as the Egfr ligands (Figure 10, Butchar *et al.* 2012). *CG4096* encodes an ADAMTS (A Dysintegrin and A Metalloproteinase with Thrombospondin Motif) protein. ADAMTS proteins in humans have been implicated in cancer, and ADAMTS1 and -15, the human orthologs of *CG4096*, have been shown to affect EGF ligands (Porter *et al*. 2006 and Wagstaff *et al*. 2011). I have conducted additional analysis in order to further characterize *CG4096*'s role in Egfr signaling.

First, I attempted to create a fly carrying a knock-out mutation of *CG4096*. Previously, an undergraduate in the Simcox lab tried to conduct a P-element excision using a transgenic fly carrying a P-element insertion in *CG4096* ($CG4096^{EPgy2}$) (Figure 1A). The excision of the P-element was successful (data not shown). However, the resulting mutation was hemizygous lethal - *CG4096* is located on the X chromosome. I performed complementation tests using transgenic flies carrying 100kb translocation/duplications of the X chromosome (Figure 1) which failed to complement the *CG4096*Δ*EPgy2* mutation.

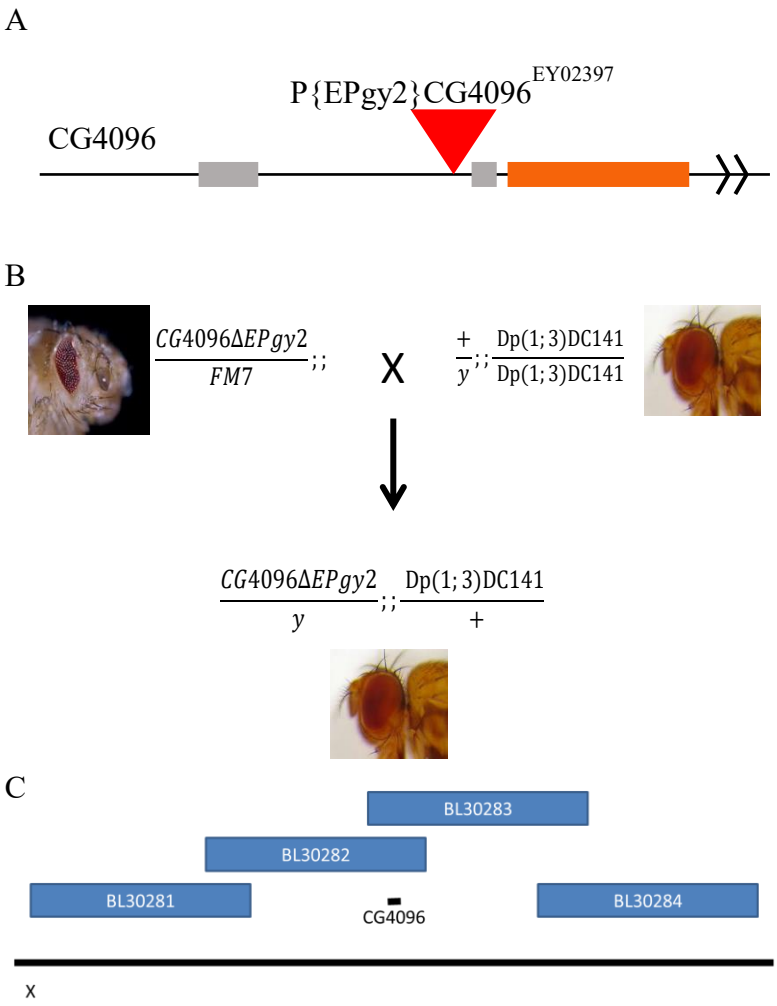

Figure 1: (A) Map of the EPgy2 P-element insertion in *CG4096*
(B) Crossing scheme for complementation test of *CG4096ΔEPgy2*
(C) X chromosome map of deletion stocks used for complementation test

Second, we used the CRISPR-Cas9 system to generate the *CG4096* mutant. CRISPR (Clustered Regularly Interspaced Short Palindromic Repeats) is a system developed from a bacterial immunological defense system used to target specific genes, while Cas9 is the protein that mediates the targeting and excision (Richter *et al*. 2012). First, we designed a guide sequence to target *CG4096* and tested it *in vitro* using Cas9-expressing Ras-attP-L1 cells generated in our lab using site-specific RMCE (Figure 2).

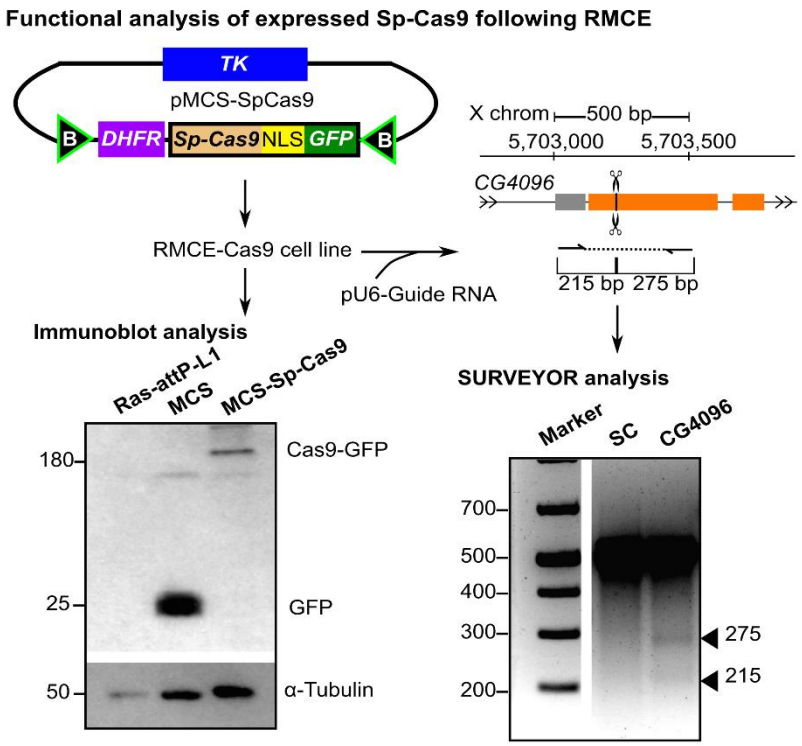

Figure 2: A Ras-attP-L1 cell line expressing a GFP-tagged Cas9 gene was generated using the RMCE protocol described in Manivannan *et al*. 2015. Western blot analysis shows the fusion protein being expressed at the correct size. These Cas9-expressing cells were transfected with a plasmid encoding a guide RNA targeting the *CG4096* gene. SURVEYOR analysis showed cleavage at the target size; a scrambled guide sequence control (SC) had no effect. (adapted from Manivannan *et al*. 2015)

After confirmation of the efficacy of our guide sequence (Figure 3), I moved to generate a mutation *in vivo*. I chose to use two guide sequences (one targeting *CG4096* and the other targeting the mini white marker) to generate a large deletion and to simplify mutant screening, as a fly carrying the correct deletion will have white eyes. The injection mixture was prepared as described in Materials and Methods, and injected into $CG4096^{EPgy2}$ flies. The injection mixture was prepared of four separate plasmids containing the following constructs, respectively: *Act-Gal4*, *UAS-Cas9-SV40*, and CRISPR plasmids (*U6-SgRNA*) targeting *CG4096* and *w* separately, and was injected

into *CG4096*^{EPgy2} flies. Unfortunately, several attempts at generating this mutant fly failed. One known culprit of the low efficiency of the system in whole flies compared to cell cultures is the use of plasmids and the requirement that transcription occurs for all components to successfully generate of a deletion. New studies show improved methods using the CRISPR/Cas9 system to create deletions in flies. Notably, CRISPR guide RNAs are injected into transgenic flies with Cas9 under *vasa* or *nanos* promoters, which allows germline expression of the enzyme (Gratz *et al*. 2015).

Finally, during my work on a genome-wide tumor suppressor screen in L.S. Shashidhara's Lab, I found that *CG4096* cooperates with *yorkie* (*yki*), a member of the Hippo signaling pathway, to generate tumor-like wing disc growth. The Hippo pathway controls organ size by regulating cell proliferation and apoptosis, and defects in this pathway have been implicated in human cancers (Zhao, B. *et al.* 2007). Co-expression of *CG4096* RNAi and *yki* (a positive regulator of the Hippo pathway), generated large tumorous wing discs in third instar larvae (Figure 4). Interestingly, co-expression of *CG4096* RNAi and *Egfr* did not show this same phenotype, even though it has been previously shown that *CG4096* interacts with *Egfr* (Figure 4, Butchar *et al*. 2012). I then looked at the cell polarity these wing discs, as loss of epithelial cell polarity can lead to metastasis of cancer (Li *et al.* 2015 and Lee and Vasioukhin 2008). However, cell polarity of actin is not lost in *ap > yki*, *CG4096*^{RNAi} wing discs (Figure 4D). It is evident that *CG4096* has a role in both the Egfr and Hippo signaling pathways, warranting further analysis into its molecular functions in *Drosophila*.

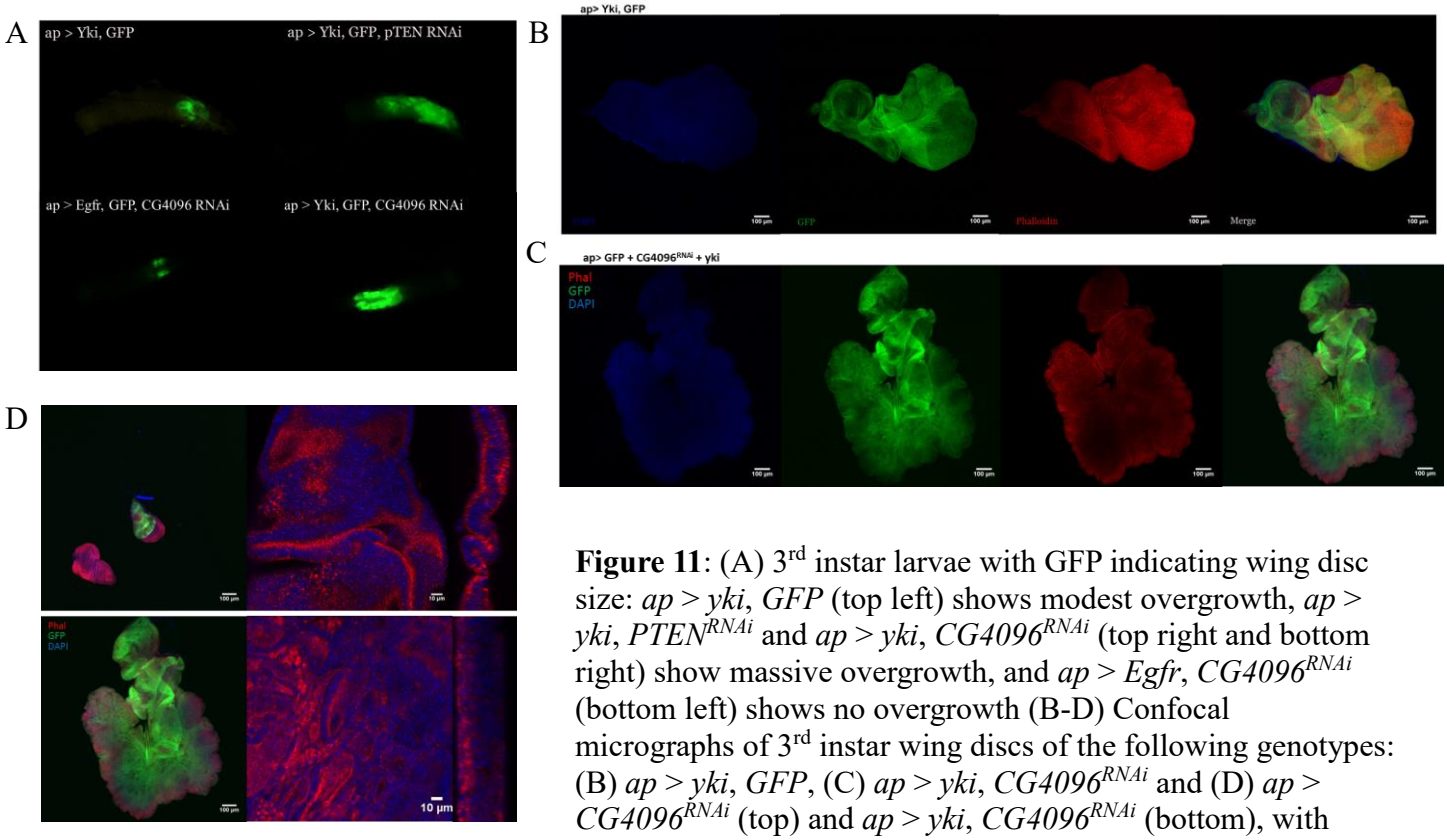

Figure 11: (A) 3rd instar larvae with GFP indicating wing disc size: *ap > yki*, *GFP* (top left) shows modest overgrowth, *ap > yki*, $PTEN^{RNAi}$ and *ap > yki*, $CG4096^{RNAi}$ (top right and bottom right) show massive overgrowth, and *ap > Egfr*, $CG4096^{RNAi}$ (bottom left) shows no overgrowth (B-D) Confocal micrographs of 3rd instar wing discs of the following genotypes: (B) *ap > yki*, *GFP*, (C) *ap > yki*, $CG4096^{RNAi}$ and (D) *ap > CG4096*^{RNAi} (top) and *ap > yki*, $CG4096^{RNAi}$ (bottom), with insets showing optical cross-section to visualize actin polarity. (L. S. Shashidhara lab, unpublished)